

REF: A0405.0407

## **HIGH TEMPERATURE BEHAVIOUR OF SIMILAR AND DISSIMILAR WELDED COMPONENTS OF STEEL GRADE P22 AND P91**

**P. Seliger<sup>1</sup>, and A. Thomas**

Siempelkamp Pruef- und Gutachter-Gesellschaft mbH

P.O. 10 02 63, D-01072 Dresden, Germany

Email: <sup>(1)</sup>[peter.seliger@siempelkamp.com](mailto:peter.seliger@siempelkamp.com)

### **SYNOPSIS**

The service of energy production plants would be impossible without the professional designing, manufacturing and monitoring of welded joints. Particularly with the increase of the steam parameters pressure and temperature the integrity of creep-exposed welded joints continues to move into the focus of the technical designers, operators and supervisors of energy-technical plants. The lifetime assessment factors of welded components, implemented in the Design Codes, must be urgently updated for the modern materials and the advanced steam parameters used in the piping construction.

### **INTRODUCTION**

Within the European research project WELDON [1] the Siempelkamp Pruef- und Gutachter-Gesellschaft mbH (SPG) is performing component-like tests at higher temperatures. On the one hand it concerns tests at inner pressurised pipes, whose circumferential weldments are stressed additionally by external axial load. The pipes from steel grade P22 and P91 are equipped with sensors for the on-line monitoring of temperatures, deformations and strains. Metallographic investigations are monitoring the damage development in the individual zones of the weld relevant for the creep strength behaviour. Further creep-rupture tests at large tensiles are accomplished, in order to be able to examine the geometry size effect. For observance of similar axial and hoop stresses pre-calculation of specimen geometry and loading have been done before manufacture. For creep testing special test rigs were designed and built. All testing data will be implemented as inputs for the numeric FE analysis. In the context of the project the determined research results flow into a methodology for the estimation of the welding seam behaviour.

### **RESULTS**

#### **2 EXPERIMENTAL DETAILS**

##### **2.1 Welding of similar and dissimilar pipe materials,**

Forged pipes of 145 mm outer diameter and 45 mm wall thickness were produced from material grades P22 and P91 according to ASTM A 369 [2]. Similar butt welds were manufactured of P22-P22 and P91-P91 as well as dissimilar butt welds of P22-P91. The dissimilar welds were welded with P22-like electrodes (2,25 % Cr).

The macro- and microstructure of the P91-P91 and P22-P91 welds are shown in Figure 1 and Figure 2.

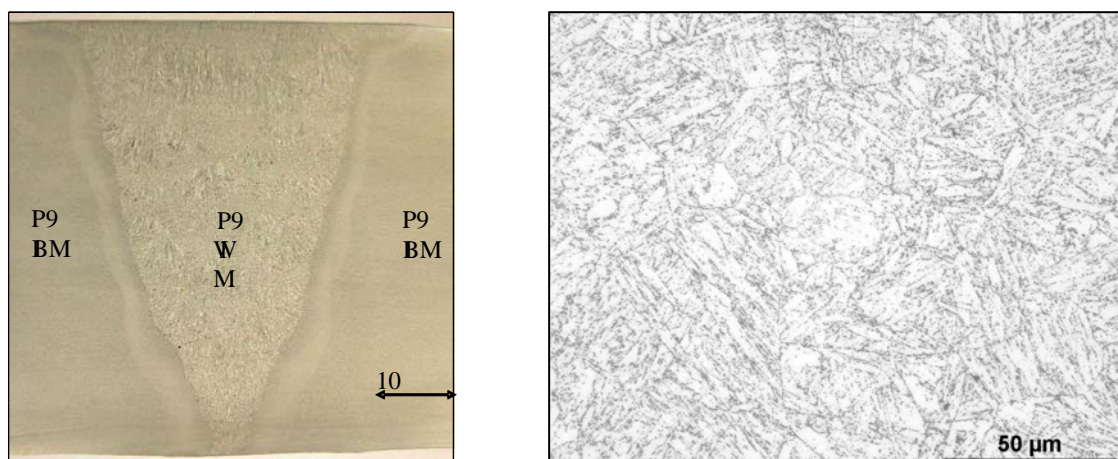


Fig. 1 Macrostructure of similar weld P91-P91, microstructure P 91 base metal (BM)

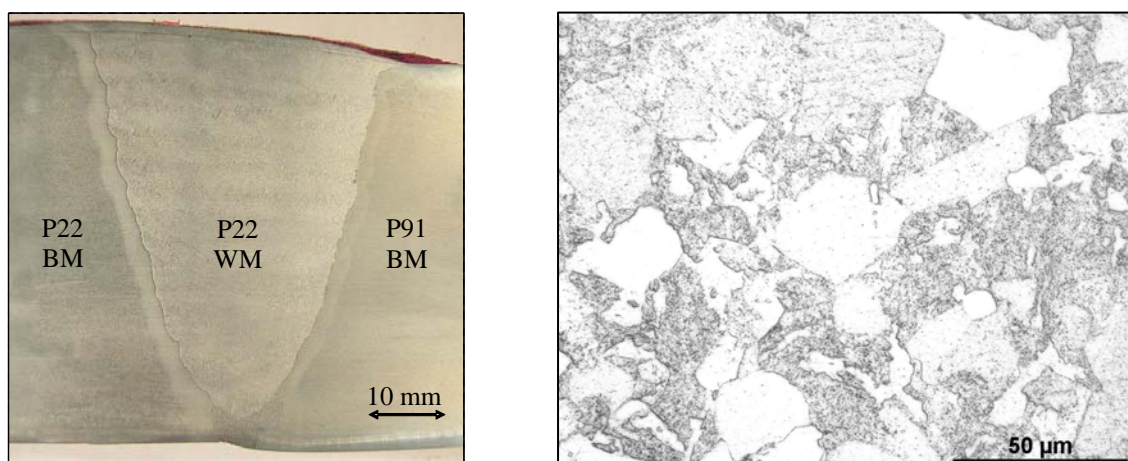


Fig. 2 Macrostructure of dissimilar weld P22-P91, microstructure P22 base metal (BM)

The microstructure of P22 pipes contains ferritic-bainitic microstructure. The microstructure of the P91 pipes show needle shaped martensite of average grain size and indicates a regular heat treatment at a sufficient austenitic temperature. All welded pipes were subjected to appropriate post weld heat treatment (PWHT). The details of welding and PWHT are presented in Table 1. After the PWHT, the pipes were examined non-destructively employing ultrasonic (UT) and Magnetic Particle Inspection (MPI) techniques, without indications for presence of welding defects or cracks.

Table 1: Details of welding technology

Joint type	Filler		Root		Post weld heat treatment
	Process	Material	Process	Material	
P22 - P22	SMAW	SHCromo2KS	GTAW	UnionICrMo910	690 °C/ 2h /air
P91 - P91	SMAW	Chromo9V	GTAW	Thermanit MTS3	760 °C/ 2h/ air
P22 - P91	SMAW	SHCromo2KS	GTAW	UnionICrMo910	725 °C/ 2h/ air

## 2.2 Finite Element Calculation

For the determination of the loading conditions finite element calculations were made. The specimen dimension and loading conditions were chosen such that the applied stresses in the hoop and axial directions (i.e. equivalent or v. Mises stress  $\sigma_v$ ) at the outer side will be the same for the pipe and will correspond to the axial load  $\sigma_a$  applied to the large tensile specimen. An open question was concerning the level of the inner pressure and loads to reach the target test times. Therefore at first an elastic FE computation of the real component was made using ANSYS. Figure 3 illustrates the FE mesh.

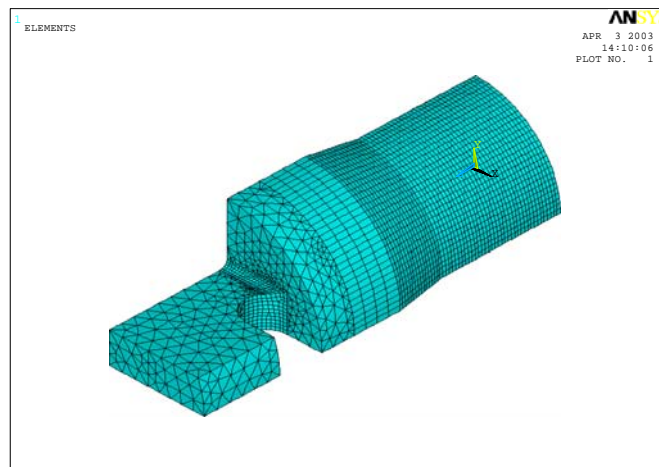


Figure 3: FE mesh

The reference stress was calculated in the weld cross section to compare the stresses with the creep rupture strength of the materials. As example, for the 10.000 hours feature test a reference stress of 85 MPa for P91-weld and about 106 MPa for P22 weld was chosen (Figure 4). This corresponds to a weld strength factor of about 85 % related to the mean value of the base material.

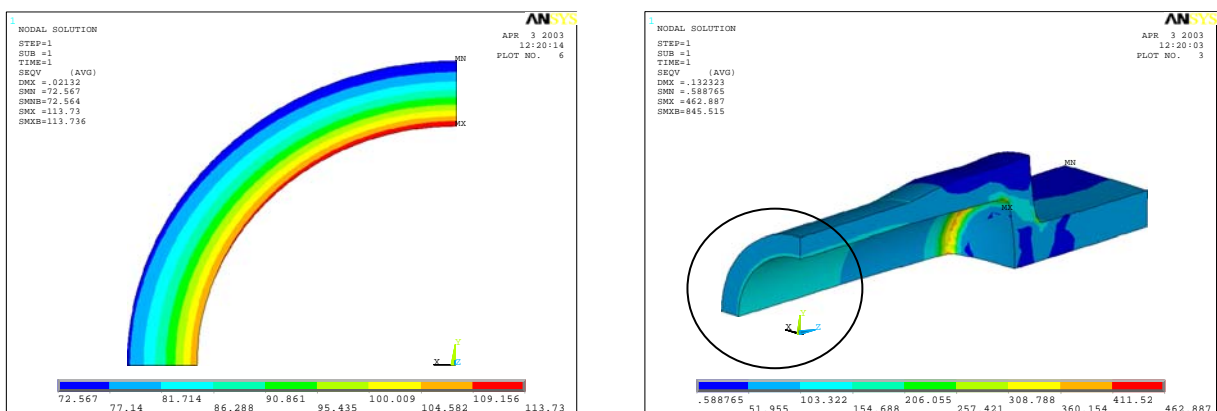


Figure 4: Calculation results of initial reference stress (equivalent stress; v. Mises)

## 2.3 Manufacture of feature test

Large tensile specimens (20 x 50 mm cross section, length 700 mm) and pipes (100 mm inner diameter, 12 resp. 15 mm wall thickness) were machined from larger welded pipes. The pre-test examination of the components includes geometrical measurements, NDE (X-ray radiography, MPI), replica examination and hardness measurements across the weld zone surface.

## 2.4 Test rig for high temperature component testing

The components are tested in specially designed high temperature test rigs (Figure 5).

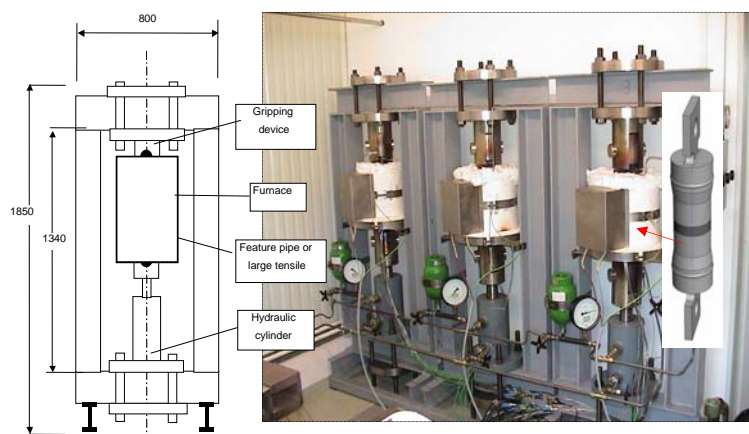


Fig. 5 High temperature test rig for pipe creep tests



Fig.6-Sensor application on test pipe P22-P91

Pipes have been tested under simultaneous application of constant internal pressure using argon and an axial loading. Electrical heating elements are used for heating the component to the test temperatures. Capacitive strain gages type HT-DMS (gage length 20 mm) were installed on the pipes to measure the integral strain on different locations (base metal BM, weld metal WM, heat affected zone HAZ) and orientations (longitudinal and circumferential), as shown in Figure 6. Additionally, a number of reference marks (creep pips) were fixed on the pipe surface for intermittent extensometer measurements during test stops. The accuracy of pressure and temperature measurements during the test duration was kept within the ECCC recommendations [3] for creep tests.

## 3 RESULTS AND DISCUSSIONS

### 3.1 Creep test and Metallographic examination

In P22-P91 dissimilar weld, a carbon/carbide depleted zone was formed due to carbon diffusion from P22 weld metal to the higher Cr containing P91 BM. This migration had led to the formation of a dark seam of carbides adjacent to the weld interface, as shown in Figure 7.

In failed P22-P91 dissimilar weld a noticeable hardness reduction was seen which is due to the decarburised zone in P22 WM, as shown in Figure 8. More microstructure data on pre-test material characterisation of feature test components are presented in [4]. Figure 9 shows the creep curves of the two large tensile specimens of P22-P91 dissimilar weld, tested at different axial loads  $\sigma_a$ . The fracture location is the decarburised zone of P22 weld metal, which corresponds to the hardness drop in figure 8.

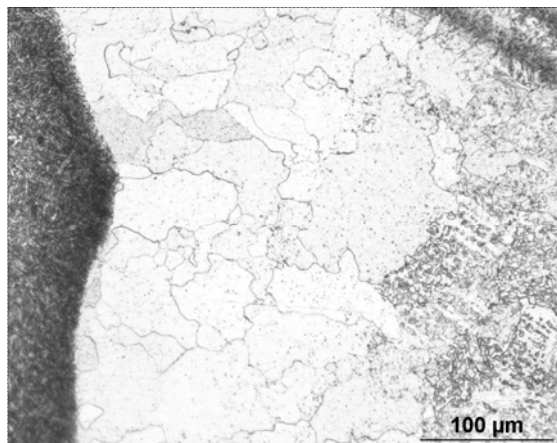


Fig. 7 P22-P91 dissimilar weld, Decarburised zone in P22 WM adjacent to P91 BM, dark carbide zone on fusion line

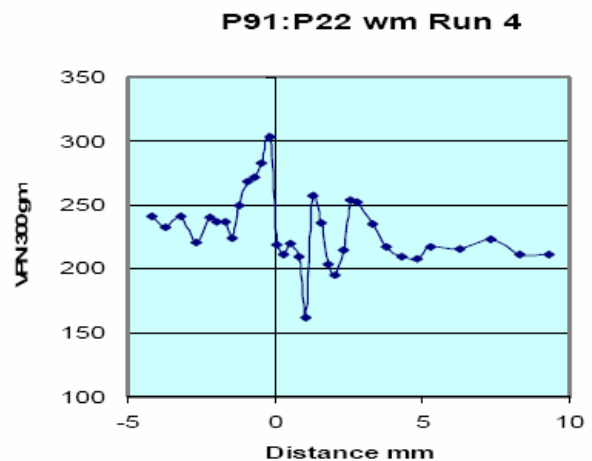


Figure 8: Hardness scan across weld, zero distance is weld interface, hardness peak in the P91 HAZ and small hardness drop in decarburised zone of P22 weld metal metal [4]

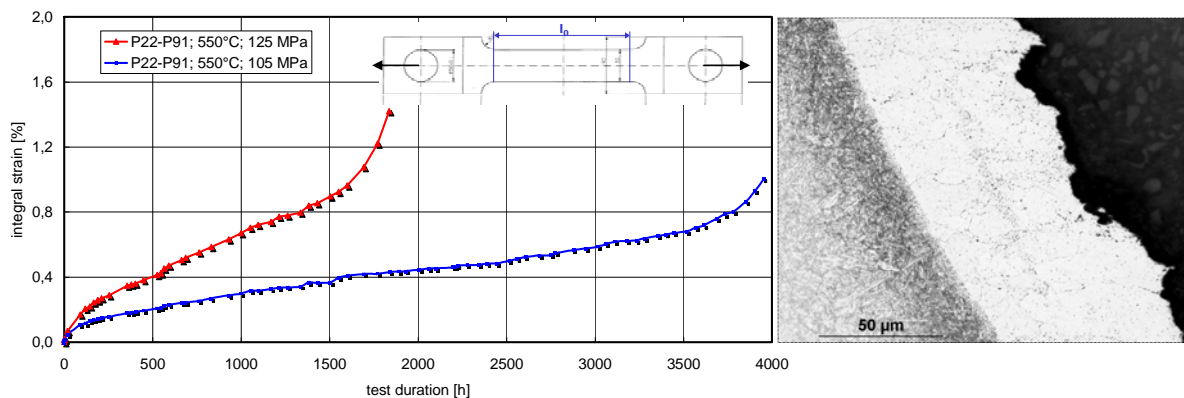


Figure 9: P22-P91 dissimilar weld, creep curves of large tensile specimens, Failure location in decarburised zone of P22-weld metal

The fracture of the large tensile specimens made from P22-P22 similar welds occurred in P22 fine grained HAZ (Type IV) after 10.191 h ( $\sigma_a=125$  MPa) and 1.276 h ( $\sigma_a=150$  MPa) of test durations, respectively.

Figure 10 illustrates the measured creep curves of the different weld zones of P91-P91 similar welded test pipe. Only the primary and secondary stages of the creep curve had been monitored by the capacitive strain gages applied on the weld surface. But, the creep crack initiation and fracture had occurred on the opposite side of the test pipe, where no sensor was installed. A small necking zone was found in circumferential direction in the HAZ where the crack had initiated (Type IV cracking).

For the P22-P22 test pipe the crack initiation and fracture was very well monitored by the strain gage fixed across the HAZ region, as indicated in Figure 11 and Figure 12. The creep curves of this sensor show the typical tertiary stage.

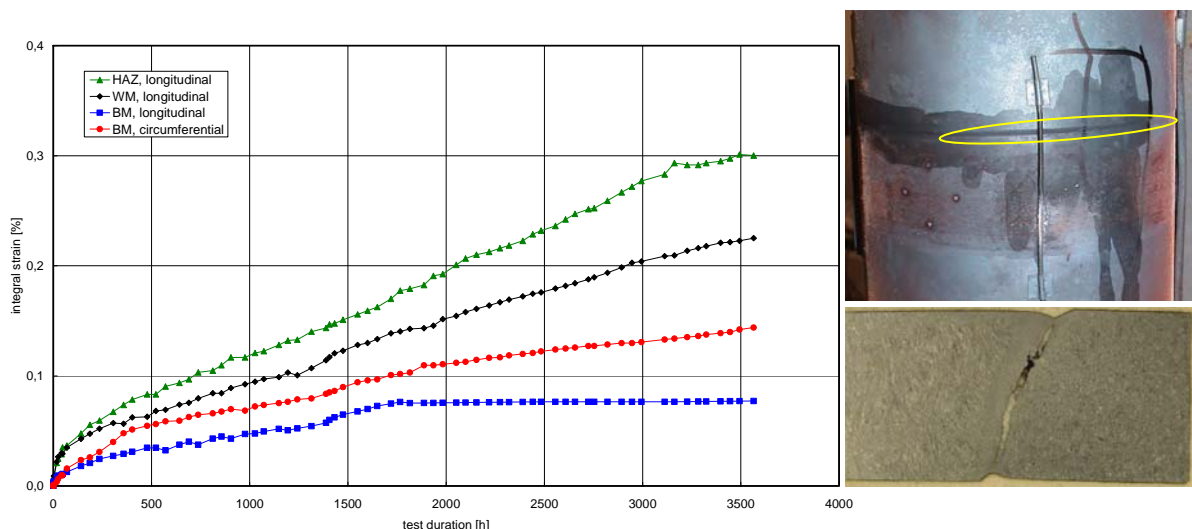


Figure 10: Pipe P91-P91 ( $\sigma_v = 102$  MPa); creep curves of different weld zones, Type IV cracking

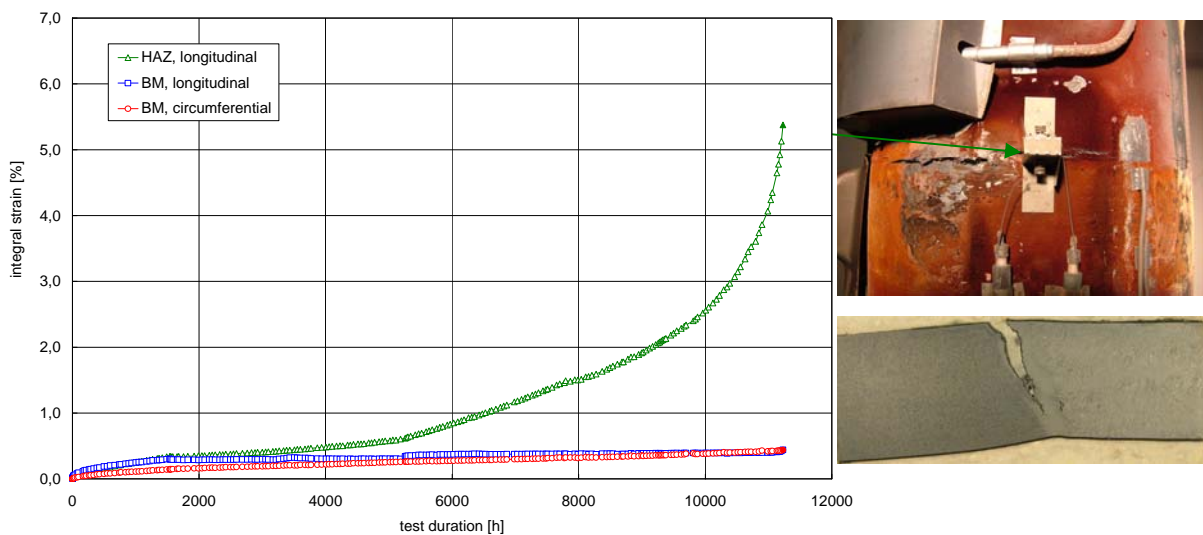


Figure 11: Pipe P22-P22 ( $\sigma_v = 128$  MPa); creep curves of different weld zones, Type IV cracking

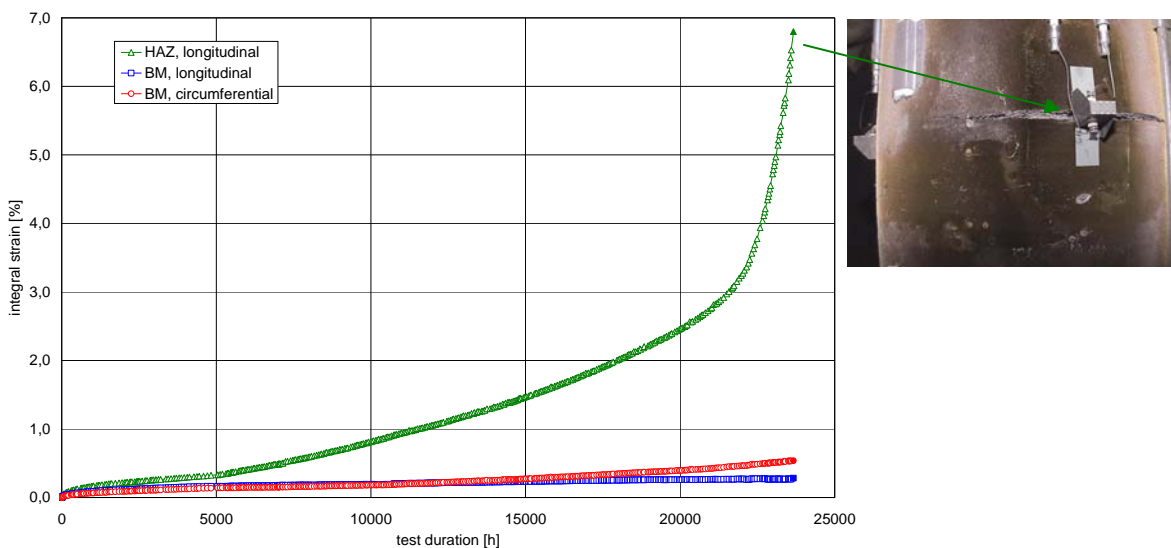


Figure 12: Pipe P22-P22 ( $\sigma_v = 106$  MPa); creep curves of different weld zones, Type IV cracking

### 3.2 Creep rupture strength – Comparison standard (uniaxial) lab tests and pipe tests

One of the main project topics was to investigate the influence of size and component type on creep rupture strength or lifetime. Figure 13 shows the results of feature tests (large tensiles/ pipes) for P22 similar weld in comparison to those of the standard uniaxial specimen, which were tested by the project partner CESI [5]. The failure points of large tensiles and standard specimens are closed together in the range of mean values of creep rupture strength. The results of the pipes seems to be better, but in the diagram the Mises-reference stress at the beginning of test is used, which leads to an overvaluation.

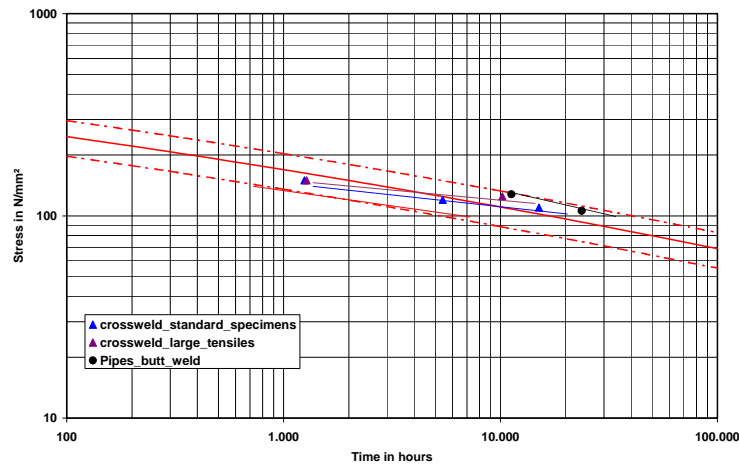


Fig. 13 Creep rupture strength, uniaxial tests and pipe tests, P22-P22 at 550 °C

It is well known, that the reference stress distribution is changing during service due to relaxation of high stressed areas. Therefore, the failure points of pipes in figure 13 should shift to lower stress levels. The amount of shifting depends on the test duration, the absolute stress level and the test temperature. The calculation of relaxation and redistribution was done by the project partner UNOTT and will be presented specially.

The crossweld standard specimens of P91 have an expected creep rupture level at the lower scatter band, like seen in figure 14. The large tensile test results are showing a non-explainable behaviour, but probably they do not differ from cross weld specimen so much.

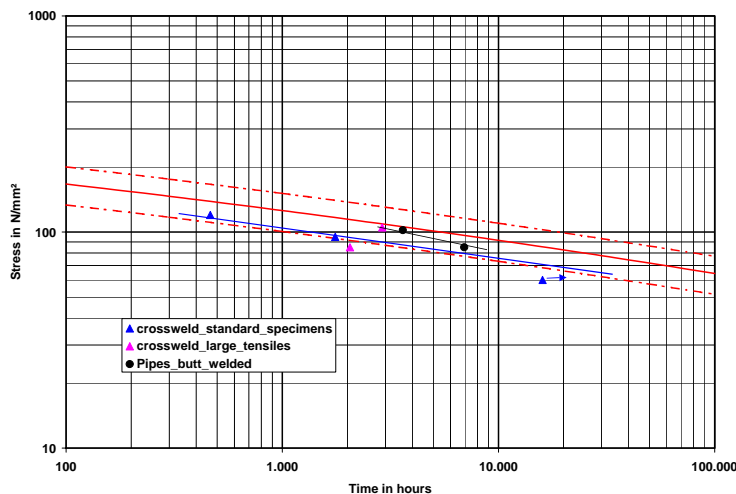


Fig. 14 Creep rupture strength, uniaxial tests and pipe tests, P91-P91 at 625 °C

For the pipes the same restrictions concerning the used reference stresses are valid like for P22-tests.

The results for the dissimilar welds P22/P91 are definitely worse than for similar P22/P22-tests. All the crossweld specimens have a strength level at the lower bound of the scatterband (Figure 15). The reason is the weakness of the decarburised zone in P22 weld metal, which is the failure location as well.

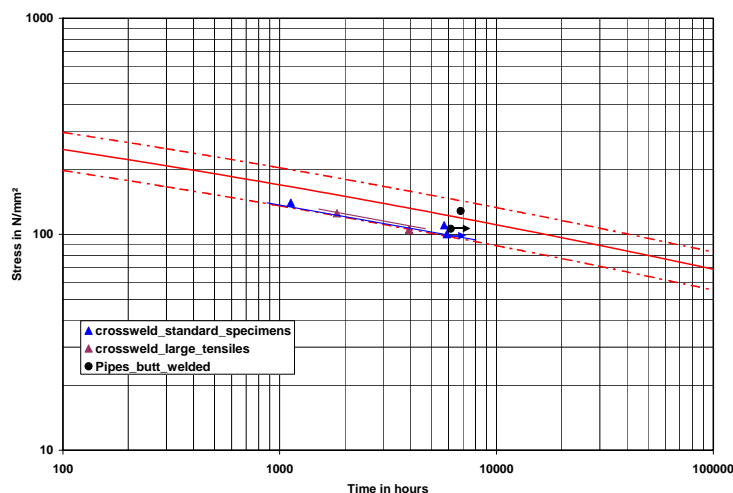


Fig. 15 Creep rupture strength, uniaxial tests and pipe tests, P22-P91 at 550 °C

#### 4 CONCLUSIONS AND OUTLOOK

Within this EU 5<sup>th</sup> Framework research project ‘WELDON’, feature tests at high temperatures are performed on component-like specimens like welded pipes and large tensile specimens in addition to laboratory specimens in order to study the geometry and size effects on the damage evaluation methodology which is being developed. The observed carbide depletion in the P22 weld metal adjacent to the fusion line of P91-P22 dissimilar welds and its effect on the weld strength reduction have to be taken into account.

No size effects or significant differences between standard crossweld and large crossweld results were observed.

The strength level of similar P22-welds at 550 °C is in the mean range of base material. On the other hand the dissimilar weld at the same temperature shows a strength at the lower bound of scatterband due to the different failure location.

Also the similar welded P91-specimens have a strength level in the range of lower scatter band, but this is due to the (for P91) very high temperature of 625 °C.

Based on the weld combinations, the component geometry and the loading conditions, the concentration of strain in the different weld regions on feature test specimens and its relation to the failure location and strain measured in standard creep testing of crossweld specimens will be investigated within the project.

#### ACKNOWLEDGMENT

The authors gratefully acknowledge the financial support provided by the European Commission to the RTD project ‘WELDON’ (Contract No. G5RD-CT-2001-00596).



## REFERENCES

1. Weld Strength for high temperature components design and operation (WELDON). European Project No. GRD2-2000-30363.
2. ASTM A 369. Standard specification for carbon and ferritic alloy steel forged and bored pipe for high-temperature service. ASTM International, 2002
3. ECCC Recommendations. Data acceptability criteria and data generation: Recommendations for creep testing of post exposed (ex-service) materials. Volume 3 Part III [Issue 2], 2001
4. Agyakwa P. Yaghi A. Becker AA. Current state of metallurgical examination of the test welds and failed notched cross weld creep samples. Report WELDON/UNOT-009/TRP-005/R0
5. S. Concari WP2 “Material supply” and WP5 “Creep tests”. CESI-Report WELDON/CESI-011/WPR-004/00